Journal of the Korean Physical Society, Vol. 60, No. 9, May 2012, pp. 1441∼1447

Stochastic Bursting Synchronization in a Population of Subthreshold Izhikevich Neurons

Sang-Yoon Kim, Youngnam Kim and Duk-Geun Hong
Department of Physics, Kangwon National University, Chunchon 200-701, Korea

Jean Kim
Wellesley College, Wellesley, Massachusetts 02481, USA

Woochang Lim*
Department of Science Education, Daegu National University of Education, Daegu 705-115, Korea

(Received 11 January 2012, in final form 16 February 2012)

We consider a population of subthreshold Izhikevich neurons that cannot fire spontaneously without noise. As the coupling strength passes a threshold, individual neurons exhibit noise-induced burstings (*i.e.*, discrete groups or bursts of noise-induced spikes). We investigate stochastic bursting synchronization by varying the noise intensity. Through competition between the constructive and the destructive roles of noise, collective coherence between noise-induced burstings is found to occur over a large range of intermediate noise intensities. This kind of stochastic bursting synchronization is well characterized by using the techniques of statistical mechanics and nonlinear dynamics, such as the order parameter, the raster plot of neural spikes, the time series of the ensemble-averaged global potential, and the phase portraits of limit cycles. In contrast to spiking neurons showing only spike synchronization (characterizing a temporal relationship between spikes), bursting neurons are found to exhibit both spike synchronization and burst synchronization (characterizing a temporal relationship between the onset times of the active phases of repetitive spikings). The degree of stochastic bursting synchronization is also measured in terms of a synchronization measure that reflects the resemblance of the global potential to the individual potential.

PACS numbers: 87.19.Lm, 87.19.Lc
Keywords: Stochastic bursting synchronization, Subthreshold neurons
DOI: 10.3938/jkps.60.1441

I. INTRODUCTION

In recent years, much attention has been paid to brain rhythms [1]. Synchronization of neural firing activities may be used for efficient sensory and cognitive processing (*e.g.*, feature integration, selective attention, working memory, and decision making) [2–4]. This kind of neural synchronization is also correlated with pathological rhythms associated with neural diseases (*e.g.*, epileptic seizures and tremors in Parkinson's disease) [5]. Here, we are interested in these synchronous brain rhythms. A neural circuit in the major parts of brain, such as the cortex, hippocampus, and thalamus, is composed of a few types of excitatory principal cells and diverse types of inhibitory interneurons [1]. The effect of chemical synapses on synchronous brain rhythms has been much investigated in neural systems composed of excitatory and/or inhibitory neurons; thus, three types of synchronization mechanisms have been found: recurrent excitation between principal cells, mutual inhibition between interneurons, and feedback between excitatory and inhibitory neurons [2, 3, 6]. Most past studies exploring mechanisms of neural synchronization were done in neural systems composed of spontaneously firing (*i.e.*, self-oscillating) suprathreshold neurons. For this case, neural synchronization occurs via cooperation of regular firings of suprathreshold self-firing neurons. Unlike the suprathreshold case, a subthreshold neuron cannot fire spontaneously without noise. Here, we are interested in collective coherence between complex noise-induced firings of subthreshold neurons. Recently, stochastic spiking synchronization (*i.e.*, collective coherence emerging via cooperation of noise-induced spikings) was observed in an excitatory [7,8] or inhibitory [9] population of subthreshold neurons. This kind of work may be thought to correspond to a "subthreshold version" of neural spiking synchronization through mutual excitation or inhibition.

*E-mail: wclim@kangwon.ac.kr

In this paper, we are concerned with another type of neural bursting activity alternating between a silent phase and an active (bursting) phase of repetitive spikings, where bursting refers a dynamical state in which a neuron repeatedly fires discrete groups or bursts of spikes [10,11]. Cortical intrinsically-bursting neurons, thalamocortical relay neurons, thalamic reticular neurons, hippocampal pyramidal neurons, and Purkinje cells in the cerebellum are representative examples of bursting neurons [12]. There are three major hypotheses on the importance of burstings [13]: (1) Burstings are necessary to overcome the synaptic transmission failure [14], (2) burstings can transmit saliency of the input because the effect of a bursting on the postsynaptic neuron is stronger than the effect of a single spike, and (3) burstings can be used for selective communication between neurons, where the interspike frequency within the bursts encodes the channel of communication [15]. Because of the ubiquity of noise in neural systems, much attention has been focused on burstings induced by noise. Noise is usually regarded as a nuisance, degrading the performance of dynamical systems. However, in certain circumstances, noise plays a constructive role in the emergence of dynamical order [16, 17]. For example, coherence resonance of noise-induced burstings in a subthreshold neuron [18], noise-induced transitions from spikings to burstings [19] and noise-induced burst synchronization in uncoupled suprathreshold neurons [19] have been reported. In contrast to such previous studies, a main subject of our study is to investigate stochastic bursting synchronization (*i.e.*, collective coherence between noise-induced burstings) in coupled systems of subthreshold neurons.

This paper is organized as follows: In Sec. II, we describe a large population of globally-coupled subthreshold Izhikevich neurons. The simple Izhikevich neuron [12,13], which produces rich firing patterns observed for many types of biological neurons such as regular spiking neurons, intrinsically bursting neurons, chattering neurons, and fast spiking neurons, is as biologically plausible as the Hodgkin-Huxley model [20], yet as computationally efficient as the integrate-and-fire model [21]. In our computational study, Izhikevich neurons interact via excitatory AMPA synapses. As the coupling strength J passes a threshold, noise-induced burstings appear in individual membrane potentials. In Sec. III, we investigate stochastic bursting synchronization by varying the noise intensity D. As D passes a lower threshold, a coherent transition occurs because of the constructive role of noise in stimulating coherence between noise-induced burstings. However, such bursting coherence disappears when D passes a higher threshold due to the destructive role of noise in spoiling the bursting coherence. Through competition between the constructive and the destructive roles of noise, stochastic bursting synchronization is found to occur over a large range of intermediate noise intensities. As in globally-coupled chaotic systems, this kind of incoherence-coherence-incoherence transition may be well described in terms of an order parameter $\mathcal{O}$ [22, 23]; for our case, the mean-square deviation of the ensemble-averaged membrane potential plays the role of $\mathcal{O}$. Furthermore, such stochastic bursting synchronization is well characterized by using the techniques of nonlinear dynamics, such as the raster plot of neural spikes, the time series of the ensemble-averaged global potential, and the phase portraits of limit cycles. Thus, bursting neurons are found to exhibit both spike synchronization (characterizing a temporal relationship between spikes) and burst synchronization (characterizing a temporal relationship between the onset times of the active phases), in contrast to spiking neurons, which show only spike synchronization. The degree of stochastic bursting synchronization is also measured in terms of a synchronization measure that reflects the resemblance of the global potential to the individual potential. Finally, a summary is given in Sec. IV.

II. A POPULATION OF SUBTHRESHOLD IZHIKEVICH NEURONS

In this section, we describe the simple Izhikevich neuron model, which is not only biologically plausible but also computationally efficient. We consider an excitatory population of N globally-coupled subthreshold Izhikevich neurons. The population dynamics in this neural network is governed by the following set of ordinary differential equations:

$$\frac{dv_i}{dt} = f(v_i) - u_i + I_{DC} + D\xi_i - I_{syn,i}, \quad (1)$$

$$\frac{du_i}{dt} = a(bv_i - u_i), \quad (2)$$

$$\frac{ds_i}{dt} = \alpha s_\infty(v_i)(1 - s_i) - \beta s_i, \quad i = 1, \cdots, N, \quad (3)$$

with the auxiliary after-spike resetting:

$$\text{if } v_i \geq v_p, \text{ then } v_i \leftarrow c \text{ and } u_i \leftarrow u_i + d, \quad (4)$$

where

$$f(v_i) = 0.04v_i^2 + 5v_i + 140, \quad (5)$$

$$I_{syn,i} = \frac{J}{N-1} \sum_{j(\neq i)}^{N} s_j(t)(v_i - V_{syn}), \quad (6)$$

$$s_\infty(v_i) = 1/[1 + e^{-(v_i - v^*)/\delta}]. \quad (7)$$

We note that $f(v)$ of Eq. (5) was obtained by fitting the spike initiation dynamics of cortical neurons so that the membrane potential v has a mV scale and the time t has a ms scale [13]. The state of the ith neuron at a time t is characterized by three dimensionless state variables: the membrane potential v_i, the recovery variable u_i representing the activation of the K^+ ionic current and the inactivation of the Na^+ ionic current, and the synaptic gate variable s_i denoting the fraction of open

synaptic ion channels. After the spike reaches its apex v_p (=30 mV), the membrane voltage and the recovery variable are reset according to Eq. (4). There are four dimensionless parameters, a, b, c, and d representing the time scale of the recovery variable u, the sensitivity of u to the subthreshold fluctuations of v, and the after-spike reset values of v and u, respectively. When the four parameters are tuned, the Izhikevich neuron model may produce 20 of the most prominent neuro-computational features of cortical neurons, such as tonic and phasic firing, threshold variability, spike latency, spike frequency adaptation, type-I and -II excitability, an integrator, and a resonator [13].

Each Izhikevich neuron is stimulated by using the common DC current I_{DC} and an independent Gaussian white noise ξ [see the 2nd and the 3rd terms in Eq. (1)] satisfying $\langle \xi_i(t) \rangle = 0$ and $\langle \xi_i(t)\ \xi_j(t') \rangle = \delta_{ij}\ \delta(t-t')$, where $\langle \cdots \rangle$ denotes the ensemble average. The noise ξ is a parametric one that randomly perturbs the strength of the applied current I_{DC}, and its intensity is controlled by the parameter D. The last term in Eq. (1) represents the coupling of the network. Each neuron is connected to all the other ones through global couplings via excitatory AMPA synapses. $I_{syn,i}$ of Eq. (6) represents a synaptic current injected into the ith neuron. Here, the coupling strength is controlled by using the parameter J, and V_{syn} is the synaptic reversal potential. We use $V_{syn} = 10$ mV for the excitatory synapse. The synaptic gate variable s obeys the 1st-order kinetics of Eq. (3) [24]. Here, the normalized concentration of synaptic transmitters, activating the synapse, is assumed to be an instantaneous sigmoidal function of the membrane potential with a threshold v^* in Eq. (7), where we set $v^* = 0$ mV and $\delta = 2$ mV. The transmitter release occurs only when the neuron emits a spike (*i.e.*, its potential v is larger than v^*). For the excitatory glutamate synapse (involving the AMPA receptors), the synaptic channel opening rate, corresponding to the inverse of the synaptic rise time τ_r, is $\alpha = 10\ \mathrm{ms}^{-1}$, and the synaptic closing rate β, which is the inverse of the synaptic decay time τ_d, is $\beta = 0.5\ \mathrm{ms}^{-1}$ [25].

Here, we consider the case of regular-spiking cortical excitatory neurons for $a = 0.02$, $b = 0.2$, $c = -65$, and $d = 8$. Depending on the system parameters, the Izhikevich neurons may exhibit either type-I or type-II excitability [12,13]; for the case of type-I (type-II) neurons, the firing frequency begins to increase from zero (non-zero finite value) when I_{DC} passes a threshold [26]. For our case, a deterministic Izhikevich neuron (for $D = 0$) exhibits a jump from a resting state [*e.g.*, see Fig. 1(a) for $I_{DC} = 3.6$] to a spiking state [*e.g.*, see Fig. 1(b) for $I_{DC} = 3.9$] via a subcritical Hopf bifurcation for $I^*_{DC,h} = 3.80$ by absorbing an unstable limit cycle born via a fold limit cycle bifurcation for $I^*_{DC,l} = 3.78$. Hence, the Izhikevich neuron (in this study) shows type-II excitability because it begins to fire with a non-zero frequency that is relatively insensitive to changes in I_{DC}, as

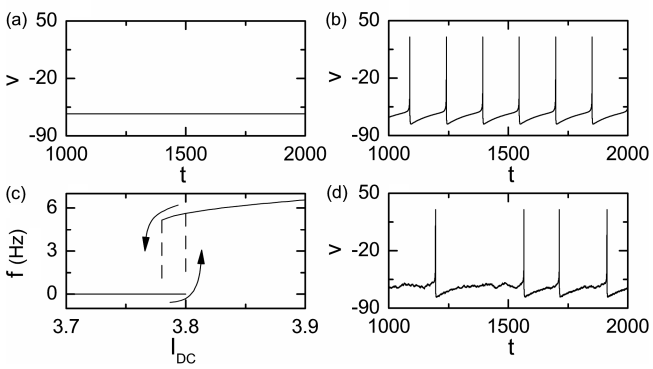

Fig. 1. Time series of the membrane potential $v(t)$ of the single Izhikevich neuron in the absence of noise ($D = 0$) for (a) $I_{DC} = 3.6$ and (b) $I_{DC} = 3.9$. (c) Plot of the mean firing rate versus I_{DC} for $D = 0$. (d) Time series of $v(t)$ for $D = 0.5$ and $I_{DC} = 3.6$.

shown in Fig. 1(c). Throughout this paper, we consider a subthreshold case of $I_{DC} = 3.6$. An isolated subthreshold Izhikevich neuron cannot fire spontaneously without noise. Figure 1(d) shows a time series of the membrane potential v of a subthreshold neuron for $D = 0.5$. Complex noise-induced subthreshold oscillations and spikings with irregular interspike intervals appear. Neural synchronization is investigated in an excitatory population of these subthreshold Izhikevich neurons coupled via AMPA synapses. Numerical integration of the governing equations, Eqs. (1) – (3), is done using the Heun method [27] (with the time step $\Delta t = 0.01$ ms), which is similar to the second-order Runge-Kutta method. For each realization of the stochastic process in Eqs. (1) – (3), we choose a random initial point $[v_i(0), u_i(0), s_i(0)]$ for the ith ($i = 1, \ldots, N$) neuron with uniform probability in the range of $v_i(0) \in (-70, 30)$, $u_i(0) \in (-10, -6)$, and $s_i(0) \in (0, 1)$.

III. STOCHASTIC BURSTING SYNCHRONIZATION

In this section, we study stochastic bursting synchronization (*i.e.*, collective coherence between noise-induced burstings). Stochastic bursting synchronization is well characterized by using the diverse techniques of statistical mechanics and nonlinear dynamics.

We consider an excitatory population of N globally-coupled subthreshold Izhikevich neurons for $I_{DC} = 3.6$. As the coupling strength J passes a threshold J^* ($\simeq 0.57$) for $D = 0.5$, individual neurons exhibit noise-induced burstings, as briefly explained below [28]. Figure 2(a1) shows the time series of the membrane potential variable v_1 and the recovery variable u_1 of the first neuron (in the population) for $J = 0.5$. The fast potential variable v_1 may exhibit a spiking or a quiescent state depending on the slow recovery variable u_1, which provides a negative

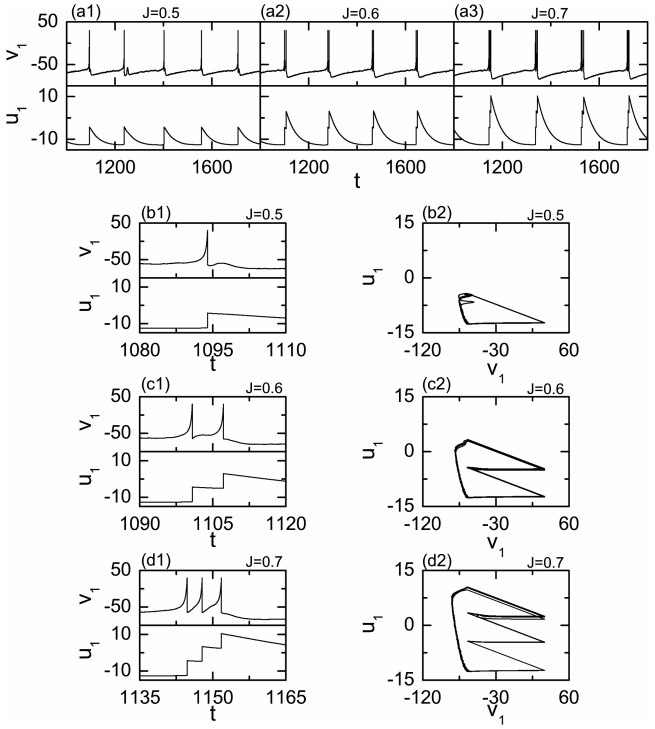

Fig. 2. Time series of the membrane potential variable v_1 and the recovery variable u_1 of the first neuron for (a1) $J = 0.5$, (a2) $J = 0.6$, and (a3) $J = 0.7$ in N $(= 10^3)$ globally-coupled excitatory subthreshold Izhikevich neurons for $I_{DC} = 3.6$ and $D = 0.5$. Magnifications of (a1), (a2), and (a3) are given in (b1), (c1), and (d1), respectively. Phase portraits projected onto the $v_1 - u_1$ plane of the first neuron for (b2) $J = 0.5$, (c2) $J = 0.6$, and (d2) $J = 0.7$.

feedback to v_1 and can be regarded as an adaptation parameter [11,12,29]. If J is less than J^* (*e.g.*, $J = 0.5$), then spiking v_1 pushes u_1 outside the spiking area. Then, u_1 slowly decays into the quiescent area [see Fig. 2(a1)], which results in termination of spiking. This quiescent v_1 pushes u_1 outside the quiescent area; then, u_1 revisits the spiking area, which leads to spiking of v_1. Through repetition of this process, spikings appear successively in v_1. This kind of spiking activity occurs on a simple limit cycle, as shown in Fig. 2(b2). However, as J passes a threshold J^*, the coherent synaptic input into the first neuron becomes so strong that the first spike in v_1 cannot push u_1 outside the spiking area. As an example, see the case of $J = 0.6$ in Figs. 2(a2) and 2(c1). For this case, after the 1st spike in v_1, u_1 at first decreases a little (with nearly zero slope) and then increases abruptly up to a value of $u_1 = 2.96$ [see Fig. 2(c1)], which is larger than the peak value of $u_1 = -4.24$ for $J = 0.5$. Thus, after the 1st spike, u_1 remains inside the spiking area; hence, a second spike appears in v_1. After this 2nd spike, u_1 is pushed away from the spiking area and slowly decays into the quiescent area, which results in the termination of repetitive spikings. In this way, burstings consisting of two spikes (doublets) appear in v_1 for $J = 0.6$. This kind

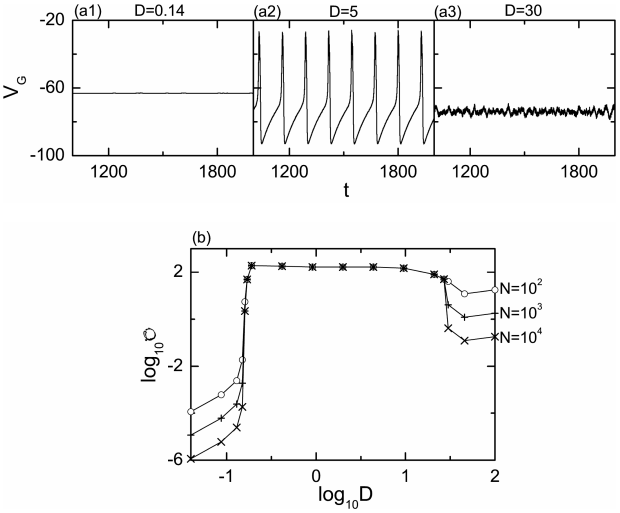

Fig. 3. Time series of the global potential $V_G(t)$ for $D =$ (a1) 0.14, (a2) 5, and (a3) 30 in N $(= 10^3)$ globally-coupled excitatory subthreshold Izhikevich neurons for $I_{DC} = 3.6$ and $J = 1.5$. (b) Plots of $\log_{10} \mathcal{O}$ versus $\log_{10} D$ for $J = 1.5$.

of bursting activity (alternating between the active phase of repetitive spikings and the quiescent phase) occurs on a hedgehog-like limit cycle (with two spines) [the spines (body) corresponds to the active (quiescent) phase], as shown in Fig. 2(c2). As J is further increased, the coherent synaptic input becomes stronger, so the number of spikes in a burst increases [*e.g.*, see the triplets for $J = 0.7$ in Figs. 2(a3), 2(d1), and 2(d2)].

Hereafter, we set the coupling strength as $J = 1.5$ and investigate stochastic bursting synchronization by varying the noise intensity D. Emergence of collective bursting coherence in the population may be described by the population-averaged membrane potential V_G (corresponding to the global potential) and the global recovery variable U_G:

$$V_G(t) = \frac{1}{N}\sum_{i=1}^{N} v_i(t) \quad \text{and} \quad U_G(t) = \frac{1}{N}\sum_{i=1}^{N} u_i(t). \quad (8)$$

For sufficiently small D, neurons fire independently, and incoherent states appear. For the incoherent case, the global potential $V_G(t)$ is nearly stationary, as shown in Fig. 3(a1) for $D = 0.14$. However, as D passes a lower threshold D_l^* $(\simeq 0.15)$, a coherent transition occurs because noise stimulates collective coherence between neural burstings. Then, stochastic bursting synchronization occurs. For this coherent case, collective oscillatory motion of the global potential $V_G(t)$ occurs [*e.g.*, see Fig. 3(a2) for $D = 5$]. However, when passing a higher threshold D_h^* $(\simeq 28)$, incoherent states appear again because noise spoils collective bursting coherence, as shown in Fig. 3(a3) for $D = 30$. This kind of incoherence-coherence-incoherence transition may be well described in terms of the order parameter. For our case, the mean-square deviation of the global potential $V_G(t)$ (*i.e.*, time-

averaged fluctuations of $V_G(t)$),

$$\mathcal{O} \equiv \overline{(V_G(t) - \overline{V_G(t)})^2}, \tag{9}$$

plays the role of an order parameter, where the overbar represents the time averaging. Here, we discard the first time steps of a stochastic trajectory as transients during 10^3 ms; then, we numerically compute $\mathcal{O}$ by following the stochastic trajectory for 3×10^4 ms when $N = 10^3, 10^4$, and 10^5. For the coherent (incoherent) state, the order parameter $\mathcal{O}$ approaches a nonzero (zero) limit value in the thermodynamic limit of $N \to \infty$. Figure 3(b) shows a plot of the order parameter versus the noise intensity. For $D < D_l^*$, the order parameter $\mathcal{O}$ tends to zero as $N \to \infty$, so incoherent states exist. As D passes the lower threshold D_l^*, a coherent transition occurs because of the constructive role of noise in stimulating coherence between noise-induced burstings. Stochastic bursting synchronization occurs in a large range of intermediate noise intensities. However, for large $D > D_h^*$, the order parameter $\mathcal{O}$ goes to zero as $N \to \infty$; hence, such coherent states disappear (*i.e.*, a transition to an incoherent state occurs when D passes the higher threshold D_h^*) due to the destructive role of noise in spoiling the spiking coherence.

We also characterize the stochastic bursting synchronization by using the techniques of nonlinear dynamics. Collective coherence between noise-induced burstings may be well visualized in the raster plots of neural spikes as shown in Figs. 4(a1) – 4(a4) for the coherent cases of $D = 0.2$, 5, 12, and 17, respectively; the time series of the corresponding global potentials $V_G(t)$ are also shown in Figs. 4(b1) – 4(b4). When passing the lower threshold D_l^* ($\simeq 0.15$), stochastic bursting synchronization occurs. For $D = 0.2$, clear burst bands, composed of stripes of spikes, appear successively at nearly regular time intervals. For a clearer view, magnifications of a single burst band and V_G are given in Figs. 4(c1) and 4(c2), respectively. For this kind of bursting, burst synchronization refers to a temporal relationship between the active phase onset and offset times of bursting neurons while spike synchronization characterizes a temporal relationship between spikes fired by different bursting neurons in their respective active phases [29,30]. Hence, bursting neurons may exhibit burst and spike synchronization in contrast to spiking neurons, which exhibit only spike synchronization. For the case of $D = 0.2$, in addition to burst synchronization, spike synchronization occurs in each burst band, as clearly shown in Fig. 4(c1). As a result of this complete synchronization, the global potential V_G exhibits a bursting activity like an individual potential (*i.e.*, fast spikes appear on a slow wave in V_G), as shown in Fig. 4(c2). This kind of bursting activity occurs on a hedgehog-like limit cycle in the $V_G - U_G$ plane [see Fig. 4(c3)]; spines of the global limit cycle indicate spike synchronization. However, as D is increased, interburst intervals decrease and loss of spike synchronization occurs in each burst band due to a smearing of

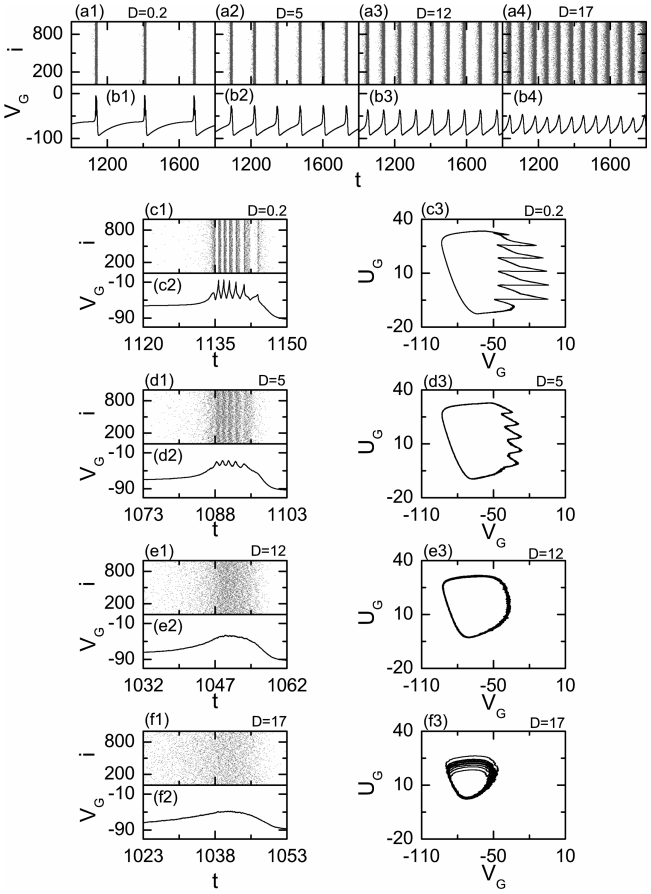

Fig. 4. Raster plots of neural spikes for D = (a1) 0.2, (a2) 5, (a3) 12, and (a4) 17 in N ($= 10^3$) globally-coupled excitatory subthreshold Izhikevich neurons for $I_{DC} = 3.6$ and $J = 1.5$. Time series of $V_G(t)$ for D = (b1) 0.2, (b2) 5, (b3) 12, and (b4) 17. Magnifications of a single burst band in the raster plot and V_G are shown in (c1) and (c2), (d1) and (d2), (e1) and (e2), and (f1) and (f2) for $D = 0.2$, 5, 12, and 17, respectively. The global phase portraits for $D = 0.2$, 5, 12, and 17 are given in (c3), (d3), (e3), and (f3), respectively.

the stripes of the spikes. As an example, see the case of $D = 5$ where the raster plot of neural spikes and V_G are given in Figs. 4(a2) and 4(b2), respectively. Smearing of the stripes is well seen in the magnified burst band of Fig. 4(d1). As a result, the amplitude of V_G decreases, as shown in Fig. 4(d2). For this case, bursting activity occurs on a smaller hedgehog-like limit cycle [see Fig. 4(d3)]. As D is further increased and passes a threshold ($D \simeq 11$), complete loss of spike synchronization occurs in each burst band. Consequently, only burst synchronization (without spike synchronization) occurs, as shown in Figs. 4(a3) and 4(b3) for $D = 12$ [see also magnified views in Figs. 4(e1) – 4(e2)]. For this case, V_G exhibits a slow-wave oscillation without fast spikes. This kind of burst synchronization occurs on a limit cycle without spines, as shown in Fig. 4(e3). As D is increased, such burst bands become more and more smeared; thus, the degree of stochastic bursting

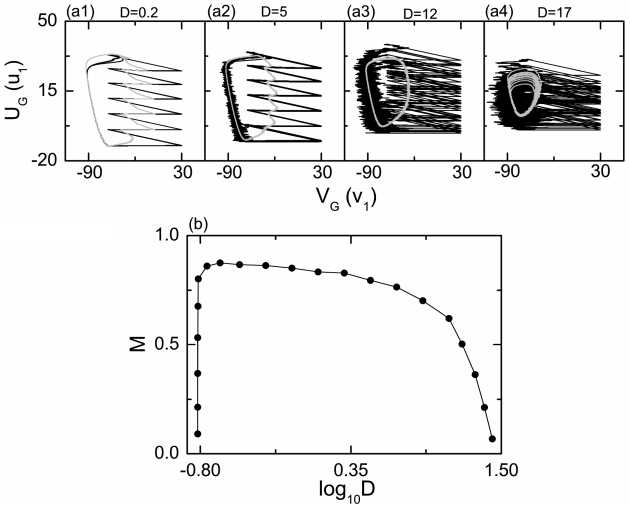

Fig. 5. Phase portraits and synchronization measure in N ($= 10^3$) globally-coupled excitatory subthreshold Izhikevich neurons for $I_{DC} = 3.6$ and $J = 1.5$. Gray (black) limit cycles of the global (first individual) state for (a1) $D = 0.2$, (a2) $D = 5$, (a3) $D = 12$, and (a4) $D = 17$. (b) Plot of the synchronization measure M versus $\log_{10} D$.

synchronization decreases [*e.g.*, see Figs. 4(a4) and 4(b4) for $D = 17$ and their magnified views in Figs. 4(f1) – 4(f2)]. Consequently, the limit cycle on which burst synchronization occurs becomes smaller, as shown in in Fig. 4(f3). With further increase in D, like the process of loss of spike synchronization, overlapping of burst bands begins to occur, which eventually results in the complete loss of burst synchronization when passing a higher threshold D_h^* ($\simeq 28$).

Finally, we measure the degree of stochastic bursting synchronization in terms of a synchronization measure. Figures 5(a1) – 5(a4) show the phase portraits of the global and the individual output signals in the coherent region. By comparing the global and the individual phase portraits, we obtain qualitative information about the degree of stochastic bursting synchronization. For $D = 0.2$, the global state exhibits a collective motion on a gray limit cycle, as shown in Fig. 5(a1). For this case, the gray limit cycle coincides nearly with the black limit cycle of the first neuron except for the spine sizes. However, as D is increased, the size of the global gray limit cycle decreases, and the width of the black limit cycle of the first neuron increases because of fluctuations in the individual output signals. In this way, with increasing D, the degree of stochastic bursting synchronization (*i.e.*, the degree of resemblance of the global output signal to the individual output signal) decreases. Such a degree of stochastic spiking coherence may be quantified by using a measure M defined by [31]

$$M \equiv \frac{\sqrt{\mathcal{O}}}{\frac{1}{N}\sum_{i=1}^{N}\sqrt{\overline{(v_i(t)-\overline{v_i(t)})^2}}}. \quad (10)$$

This synchronization measure M is just the ratio between the standard deviation (*i.e.*, the root-mean-square deviation) of the global potential V_G and the population average over each neuron's standard deviation of the individual potential v_i (*i.e.*, M reflects the degree of resemblance of the global potential to the individual potential). For the case of a coherent state, $0 < M \leq 1$, while $M = 0$ in the case of an incoherent state. Here, we numerically compute M by following the stochastic trajectory for 3×10^4 ms after a transient process of 10^3 ms. Figure 5(b) shows a plot of M versus the noise intensity. As D is increased from the lower threshold D_l^*, M increases dramatically at first, indicating the onset of bursting synchronization; then a wide plateau with nearly constant M follows. However, for larger D, M decreases due to the destructive role of noise in spoiling the bursting synchronization. Thus, stochastic bursting synchronization becomes stable over a large range of intermediate noise intensities.

IV. SUMMARY

We have studied stochastic bursting synchronization by varying the noise intensity D in a population of subthreshold Izhikevich neurons. As the coupling strength passes a threshold, individual neurons exhibit noise-induced burstings. Through competition of the constructive and the destructive roles of noise, collective coherence between these noise-induced burstings has been found to occur over a large range of D. This stochastic bursting synchronization has been well characterized in terms of the order parameter, the raster plot of neural spikes, the time series of the ensemble-averaged global potential, and the phase portraits of limit cycles. In contrast to spiking neurons showing only spike synchronization, two kinds of spike and burst synchronization are found to occur for the case of bursting neurons. We have also measured the degree of stochastic bursting synchronization by using a synchronization measure that reflects the resemblance of the global potential to the individual potential. Finally, we note that stochastic bursting synchronization might be associated in a noisy environment with synchronous brain rhythms that contribute to cognitive functions such as information integration, working memory, and selective attention.

ACKNOWLEDGMENTS

S.Y.K. completed the final version of the manuscript during his visit to Jeju National University, and he thanks Profs. D. Kang and D. Kim for their hospitality.

REFERENCES

[1] G. Buzsáki, *Rhythms of the Brain* (Oxford University Press, New York, 2006).
[2] X. J. Wang, Physiol. Rev. **90**, 1195 (2010).
[3] N. Brunel and V. Hakim, Chaos **18**, 015113 (2008).
[4] C. M. Gray, J. Comput. Neurosci. **1**, 11 (1994).
[5] B. Hauschildt, N. B. Janson, A. Balanov and E. Schöll, Phys. Rev. E **74**, 051906 (2006); P. Grosse, M. J. Cassidy and P. Brown, Clin. Neurophysiol. **113**, 1523 (2002); P. Tass, M. G. Rosenblum, J. Weule, J. Kurths, A. Pikovsky, J. Volkmann, A. Schnitzler and H. J. Freud, Phys. Rev. Lett. **81**, 3291 (1998).
[6] X. J. Wang, *Encyclopedia of Cognitive Science*, edited by L. Nadel (MacMillan, London, 2003), p. 272.
[7] Y. Wang, D. T. W. Chik and Z. D. Wang, Phys. Rev. E **61**, 740 (2000).
[8] W. Lim and S. Y. Kim, J. Korean Phys. Soc. **51**, 1427 (2007); Int. J. Mod. Phys. B **23**, 703 (2009).
[9] W. Lim and S. Y. Kim, J. Comput. Neurosci. **31**, 667 (2011); D. G. Hong, S. Y. Kim and W. Lim, J. Korean Phys. Soc. **59**, 2840 (2011).
[10] *Bursting: The Genesis of Rhythm in the Nervous System*, edited by S. Coombes and P. C. Bressloff (World Scientific, Singapore, 2005).
[11] E. M. Izhikevich, Int. J. Bifurcat. Chaos **10**, 1171 (2000).
[12] E. M. Izhikevich, *Dynamical Systems in Neuroscience* (MIT Press, Cambridge, 2007).
[13] E. M. Izhikevich, IEEE Trans. Neural Networks **14**, 1569 (2003); *ibid.* **15**, 1063 (2004); E. M. Izhikevich and G. M. Edelman, Proc. Natl. Acad. Sci. U.S.A. **105**, 1063 (2008).
[14] J. Lisman, Trends Neurosci. **20**, 38 (1997).
[15] E. M. Izhikevich, N. S. Desai, E. C. Walcott and F. C. Hoppensteadt, Trends Neurosci. **26**, 161 (2003).
[16] B. Lindner, J. Garcia-Ojalvo, A. Neiman and L. Schimansky-Geier, Phys. Rep. **392**, 321 (2004).
[17] F. Moss, L. M. Ward and W.G. Sannita, Clin. Neurophysiol. **115**, 267 (2004); L. Gammaitoni, P. Hänggi, P. Jung and F. Harchesoni, Rev. Mod. Phys. **70**, 223 (1998).
[18] A. Longtin, Phys. Rev. E **55**, 868 (1997).
[19] X. Lang, Q. Lu and J. Kurths, Phys. Rev. E **82**, 021909 (2010); A. B. Neiman, T. A. Yakusheva and D. F. Russell, J. Neurophysiol **98**, 2795 (2007); A. B. Neiman and D. F. Russell, Phys. Rev. Lett. **88**, 138103 (2002).
[20] A. L. Hodgkin and A. F. Huxley, J. Physiol. **117**, 500 (1952).
[21] L. Lapicque, J. Physiol. Pathol. Gen. **9**, 620 (1907); L. F. Abbott, Brain Res. Bull. **50**, 303 (1999).
[22] S. J. Baek and E. Ott, Phys. Rev. E **69**, 066210 (2004); D. Topaj, W. H. Kye and A. Pikovsky, Phys. Rev. Lett. **87**, 074101 (2001); H. Sakaguchi, Phys. Rev. E **61**, 7212 (2000).
[23] S. C. Manrubia, A. S. Mikhailov and D. H. Zanette, *Emergence of Dynamical Order* (World Scientific, Singapore, 2004).
[24] D. Golomb and J. Rinzel, Physica D **72**, 259 (1994); X. J. Wang and G. Buzsáki, J. Neurosci. **16**, 6402 (1996).
[25] C. Börgers and N. Kopell, Neural Comput. **15**, 509 (2003); *ibid.* **17**, 557 (2005).
[26] A. L. Hodgkin, J. Physiol. **107**, 165 (1948); J. Rinzel and B. Ermentrout, *Methods in Neural Modeling: from Ions to Networks*, edited by C. Koch and I. Segev (MIT Press, Cambridge, 1998), p. 251.
[27] M. San Miguel and R. Toral, *Instabilities and Nonequilibrium Structures VI*, edited by J. Martinez, R. Tiemann and E. Tirapegui (Kluwer Academic Publisher, Dordrecht, 2000), p. 35.
[28] More rigorous analysis for the appearance of burstings is beyond the scope of this paper. Such a rigorous investigation is left as a future work.
[29] I. Omelchenko, M. Rosenblum and A. Pikovsky, Eur. Phys. J. Spec. Top. **191**, 3 (2010).
[30] J. E. Rubin, Scholarpedia **2**, 1666 (2007).
[31] D. Hansel and G. Mato, Neural Comput. **15**, 1 (2003); D. Golomb and J. Rinzel, Physica D **72**, 259 (1994).